

# IP ORBIT CORRECTION UPDATE FOR HL-LHC\*

D. Gamba<sup>†</sup>, R. De Maria, CERN, Geneva 1217, Switzerland

## Abstract

The HL-LHC design foresees a substantial modification of the LHC layout next to the low beta Interaction Points (IPs), namely IP1 and IP5. The inner triplets will be replaced by larger aperture ones to achieve lower beta at the IPs and crab cavities (CCs) will be installed. This will add new constraints to the orbit control, which required a careful choice of location and strength of the new orbit correctors to be installed in the area. The new orbit correction system will need to correct for the unavoidable imperfections, but also provide the necessary flexibility for implementing and optimising the crossing scheme. Detailed studies of the HL-LHC layout versions HLLHCV1.0 and HLLHCV1.1 were already performed. This paper is the continuation of these works and is based on the latest layout HLLHCV1.3. A simplification of the previous analysis is proposed that helps to identify the dominant imperfections. The expected performance and tolerances of the present layout are presented.

## INTRODUCTION

An extensive study on the orbit corrector requirements for HL-LHC was already published in [1]. The present document is an update that takes into account the most recent baseline [2] and its latest evolutions.

For the purpose of this paper, we consider only the Long Straight Sections (LSS) that host the high-luminosity experiments, namely ATLAS and CMS, located at IP1 and IP5. Thanks to the symmetry of the machine we discuss only the right side of the IP5. The other IP/side informations can be recovered by applying the following symmetries:

- left IP side for Beam 1 (B1) is equal to right IP side for Beam 2 (B2);
- horizontal plane of IP5 is equal to vertical plane of IP1.

The following section presents the method used for the analysis, followed by the analysis of the present baseline HLLHCV1.3.

The naming conventions used in the following figures and tables are the one used in the MAD-X [3] model of LHC/HL-LHC. For example, the “MCBYH.B4R5.B1” is the second (B) horizontal (H) orbit corrector (MC) of type MCBY installed next to Q4 (4) on the right (R) side of IP5 (5) acting on beam 1 (B1). Similarly, its normalized strength is called “ACBYH4.R5B1”, where (A) stands for angle.

## ANALYSIS METHOD

The analysis assumes a fully linear machine, i.e. composed only by perfect quadrupoles and orbit correctors. In the LSS the only non-linear elements are the non-linear

correctors mainly used to compensate for the unavoidable imperfections of the adjacent magnets, which we neglect for the purpose of this study. Under those assumptions one can treat the problem mainly using two linear relations:

$$\vec{\Delta x} = \mathbf{RM}_c \vec{\Delta c} \quad (1)$$

$$\vec{\Delta x} = \mathbf{RM}_e \vec{\Delta e} \quad (2)$$

where  $\vec{\Delta x}$  is the beam orbit variation at the various machine locations and  $\mathbf{RM}_{c/e}$  are the respective orbit response matrices for corrector strength variations ( $\vec{\Delta c}$ ) and element imperfections ( $\vec{\Delta e}$ ). The quest for operational knobs, e.g. to steer the beam at some given location identified by a  $\dagger$ , is solved by simply inverting a sub-set of rows of Eq. (1):

$$\vec{\Delta c}_{knob} = \text{pinv}(\mathbf{RM}_c^\dagger) \vec{\Delta x}^\dagger. \quad (3)$$

Similarly, the orbit corrector strengths required for correcting for the various machine imperfections is computed as:

$$\vec{\Delta c}_{imp.} = -\text{pinv}(\mathbf{RM}_c^\dagger) \mathbf{RM}_e^\dagger \vec{\Delta e} = \mathbf{A} \vec{\Delta e}. \quad (4)$$

In both cases the (pseudo-)inversion “ $\text{pinv}(\mathbf{RM}_c^\dagger)$ ” can be computed via a Singular Value Decomposition (SVD) [4] of  $\mathbf{RM}_c^\dagger$  which can be used to solve the problem in a least-square sense. For under-constrained cases (e.g. more correctors than constraints) the null space of  $\mathbf{RM}_c^\dagger$  can be used to shift the corrector strength from one corrector to another to try finding a solution within the corrector strength limits.

One might also be interested in knowing the residual orbit at all machine locations. For machine imperfection this is computed as:

$$\vec{\Delta x} = \left[ \mathbf{RM}_e - \mathbf{RM}_c \text{pinv}(\mathbf{RM}_c^\dagger) \mathbf{RM}_e^\dagger \right] \vec{\Delta e} = \mathbf{B} \vec{\Delta e}. \quad (5)$$

The matrices  $\mathbf{A}$  and  $\mathbf{B}$  identified in Eq. (4) and (5) allow to estimate the impact of each imperfection (i.e. each matrix column) on the required corrector strengths and the residual machine orbit, respectively. The maximum strength required for the  $i$ -th corrector in the worst case scenario can be computed as:

$$\max(\Delta x_i) = \sum_j |\mathbf{A}_{ij}| \max(|\Delta e_j|) \quad (6)$$

where  $\max(|\Delta e_j|)$  is the expected maximum amplitude of the  $j$ -th imperfection. The covariance matrix of the needed corrector strengths,  $\Sigma_c$ , can also be estimated from a given covariance matrix of the errors,  $\Sigma_e$ , as

$$\Sigma_c = \mathbf{A} \Sigma_e \mathbf{A}^T \quad (7)$$

By definition, the square root of the diagonal elements of  $\Sigma_c$  gives the required r.m.s. strength for each corrector. Analogue equations can be written using matrix  $\mathbf{B}$  to obtain the

\* Research supported by the HL-LHC project

<sup>†</sup> davide.gamba@cern.ch

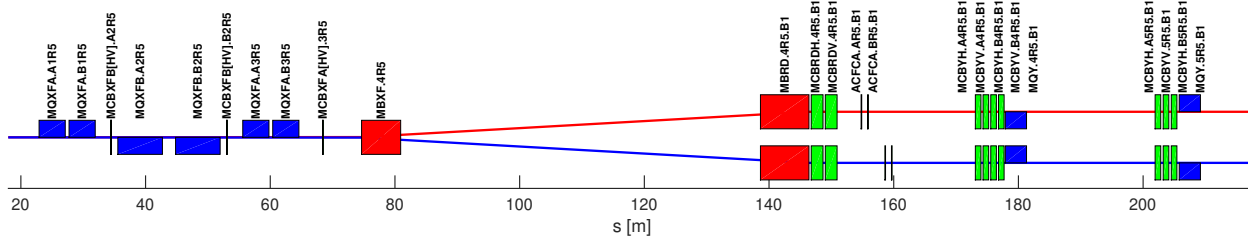


Figure 1: Layout of the right side of IP5 up to Q5 according to the present HL-LHC baseline. Only quadrupoles (MQ\*), separation and recombination dipoles (MB\*), orbit correctors (MC\*) and crab cavities (AC\*) are depicted at their nominal longitudinal position with respect to IP5. The transverse dimensions are not to scale.

maximum and variance of the residual orbit. Note that the worst scenario, Eq. (6) would be strongly pessimistic. A more realistic quantity is the r.m.s. eventually multiplied by a factor 2 margin (value identified by comparing the results obtained by same method with the actual operational LHC configurations [5]). This will be the quantity given as a result of the following analysis.

The response matrices  $\mathbf{RM}_{c/e}$  depends only on the machine layout and beam optics in use, and can be easily computed with MAD-X. The fully squeezed round collision optics (15 cm  $\beta^*$  at 7 TeV beam energy) [6] is the most sensitive to misalignments and demanding in terms of orbit corrector strengths among the HL-LHC baseline optics. Therefore only this optics is considered in the following.

## BASELINE LAYOUT

Figure 1 shows the present baseline HL-LHC orbit corrector layout, which is designed to:

- implement the beam orbit crossing angle (up to  $\pm 295 \mu\text{m}$ ) in one plane (e.g. horizontal) and separation bump (up to  $\pm 0.75 \text{ mm}$ ) in the other plane (e.g. vertical), compatible with potential (non baseline) swap of crossing and separation planes;
- control the beam orbit at the CCs ( $\pm 1 \text{ mm}$ ) independently from the IP, compatible with potential (non baseline) installation of 2 additional CCs per IP side/beam ( $\pm 0.5 \text{ mm}$  orbit adjustment at the second pair of CCs);
- correct for the expected quadrupole misalignments and dipole tilt and transfer function errors;
- adjust the IP position (up to  $\pm 2 \text{ mm}$ ), due to the experienced tracker detector misalignment with respect to the accelerator elements, with no need of hardware components realignment, besides the CCs;
- allow for small adjustment of the beam position at the IP ( $\pm 100 \mu\text{m}$ , independently for both beams) for luminosity optimisation.

Note that the HL-LHC, Q4 will be a newly designed cold mass associated with four orbit correctors per aperture. The present LHC Q4 assembly (quadrupole plus orbit correctors) is expected to be used as the future HL-LHC Q5. All magnets in the IR from Q1 to D1 (MBXF) and D2 (MBRD) with its orbit correctors (MCBRD) will be completely new magnets [2]. The introduction of the Crab Cavities is one of the

key component of the HL-LHC design, and their tight orbit requirements ( $< \pm 0.5 \text{ mm}$  at full voltage and beam loading, after removing the misalignment tolerances inside the cryomodule [7]) justify the presence of additional correctors in their proximity.

## Baseline Knobs

Figure 2 shows the horizontal orbit on the right side of IP5 under the effect of the knobs foreseen by the HL-LHC baseline. Note that the “2 crabs offset” knob requires an orbit

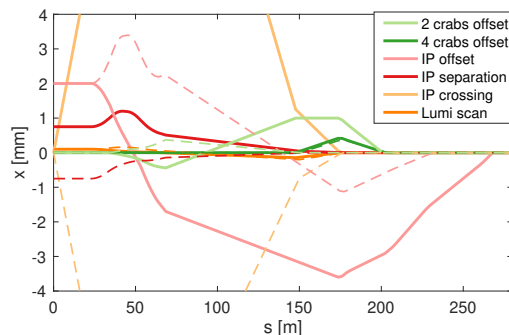


Figure 2: B1 (solid) and B2 (dashed) horizontal orbit as a function of the distance from IP5 under the effect of the individual orbit knobs. For the separation knob (red) the vertical orbit is given instead of the horizontal one. The IP crossing knob reaches up to 15 mm orbit at  $s \approx 65 \text{ m}$ .

leakage inside the IR, while the “IP offset” knob introduces a significant (up to 3.5 mm) orbit bump which is closed only at Q7 ( $s \approx 260 \text{ m}$ ) including the CCs. The IP crossing knob induces an orbit of about 0.5 mm at the CCs ( $s \approx 160 \text{ m}$ ), asymmetric for the two beams. Since the CCs are expected to tolerate only up to 0.5 mm beam orbit, they will need to be voluntary misaligned in order to be centered on the beam according to the chosen IP crossing scheme and IP shift.

## Impact of Imperfections

The following imperfections are considered:

- $\pm 0.5 \text{ mm}$  transverse quadrupole misalignments;
- $\pm 10 \text{ mm}$  longitudinal quadrupole and dipole shifts;
- $\pm 0.002$  relative strength error for quadrupoles (DKR1) and dipoles (DKR0);

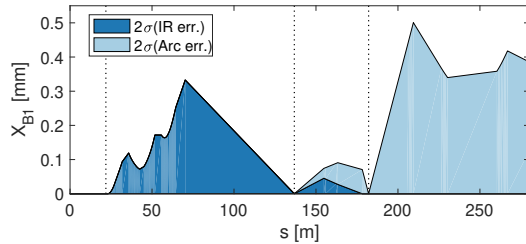


Figure 3:  $2 \times$  r.m.s. residual B1 horizontal orbit on the right side of IP5 after correcting for the expected imperfections. The dotted lines highlight the BPMs used for the correction.

- $\pm 1$  mrad roll for quadrupoles and  $\pm 0.5$  mrad for dipoles.

The values above have to be intended as boundaries of a square distribution, therefore the r.m.s. of each imperfection ( $\sigma_{e_i}$ ) is given by the assumed max divided by  $\sqrt{3}$ . Under the assumption of zero correlation between different errors, the covariance matrix of the error distribution is a diagonal matrix of all  $\sigma_{e_i}^2$ .

For all errors we assume to correct to an ideal zero the residual orbit at the first Beam Position Monitors (BPMs) next to the IP and the CCs and not to leak any orbit in the arcs adjacent to the LSS. Such a system would be heavily under-determined, but adding weights to Eq. (4) it is possible to minimise the residual orbit along the whole LSS BPMs and therefore minimise the aperture losses. Figure 3 shows the  $2 \times$  r.m.s. residual orbit after correcting for the above imperfections. The impact of IR elements (from Q1 to D1) and arc (from D2) imperfections are shown separately. The aperture loss results to be less than 0.5 mm. Note the residual orbit of less than 100  $\mu$ m at the CCs ( $s \approx 160$  m). This could be reduced by using the CC beam loading signal as a BPM. This analysis can contribute to reduce the budget allocated in aperture estimates currently set to  $\pm 2$  mm [8]. Also note that accuracy and possible misalignment of the BPMs have not been considered here.

### Required Corrector Strength

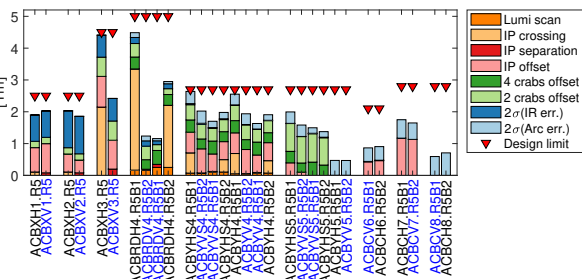


Figure 4: Stacked absolute corrector strength required to implement the presented knobs (shades of red and green) and to correct for magnets imperfections (shades of blue). Red triangles indicate the available corrector strengths.

Figure 4 summarises the orbit corrector strengths required for implementing all knobs and for correcting the machine

imperfections. Each contribution can be summed up directly since all knobs are independent and could either be positive or negative.

The IP offset and CC offset knobs require a considerable amount of corrector strengths spread up to Q7. By design all the IP-related knobs are made as close as possible to the IP with the aim of minimising the aperture loss in the MS and the leakage orbit at the CCs. The impossibility of closing the IP crossing knob with the MCBRDs (i.e. before the CCs) is due to the limited strength of the MCBXFA in Q3.

## OPTIMISED LAYOUT

Presently, an alternative machine layout is being considered: by profiting of an upgraded version of the HL-LHC remote alignment system [9] it could be possible to reuse the existing Q4 and Q5 cold masses cooled at 4.5 K as in the LHC [10]. For such a machine the available and used corrector strengths are presented in Fig. 5. Here the IP offset knob

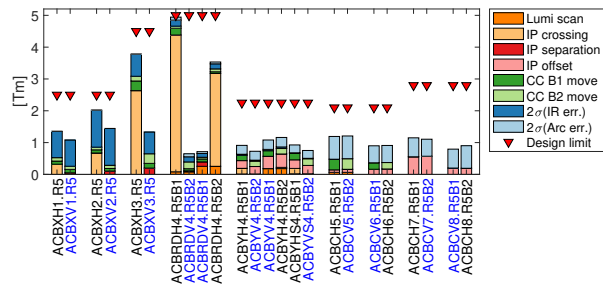


Figure 5: As Fig. 4, but for an alternative HL-LHC layout.

would be implemented by voluntarily displacing (still up to  $\pm 2$  mm) all elements from Q4 left to Q4 right, and by an orbit bump localised between Q4 and Q8. It is also assumed that the orbit adjustability at the CCs could also be reduced to  $\pm 0.5$  mm, and that the remote alignment system could be used to zero the impact on orbit (and corrector strength) of quadrupole transverse misalignments (up to Q5). The freed orbit corrector strength would allow to further reduce the orbit leakage at the CCs for implementing the IP crossing knob. Another big advantage would be a wider available aperture in the IR. On the other hand, such a layout would require a full deployment of the remote alignment system to be used at least with a safe beam circulating in the machine.

## CONCLUSIONS

A simplified method for analysing and optimising the use of the HL-LHC orbit correctors has been put in place. The available corrector strength in HLLHCv1.3 is sufficient to implement the necessary knobs and to compensate for the expected machine imperfections. Those results are compatible with the studies on previous layout/optics versions [1].

A fully remote alignment system could reduce the required orbit corrector strength and orbit leakage leading to a simplification of the matching section. Studies to verify the feasibility and cost of such an option are ongoing.

## REFERENCES

- [1] M. Fitterer *et al.*, “Crossing scheme and orbit correction in IR1/5 for HL-LHC”, Geneva, Switzerland, Rep. CERN-ACC-2015-0014, Jan. 2015.
- [2] G. Apollinari (ed.) *et al.*, “High-Luminosity Large Hadron Collider (HL-LHC): Technical Design Report V. 0.1”, Geneva, Switzerland, Rep. CERN-2017-007-M, 2017.
- [3] MAD-X, <http://mad.web.cern.ch/mad/>.
- [4] G. Golub, W. Kahan, “Calculating the Singular Values and Pseudo-Inverse of a Matrix”, *Journal of the Society for Industrial and Applied Mathematics Series B Numerical Analysis*, vol. 2, pp. 205–224, Jul. 1965.
- [5] R. De Maria, “Can we simplify the correctors and magnet circuits for HL-LHC?”, presented at the LHC Performance Workshop 2017, Tuesday, 26 Jan. 2017, <https://indico.cern.ch/event/580313/contributions/2359640/>.
- [6] HL-LHC round collision optics v. 1.3, [http://cern.ch/lhc\\_optics\\_web/www/hllhc13/round15/](http://cern.ch/lhc_optics_web/www/hllhc13/round15/)
- [7] P. Baudrenghien, R. Calaga, “Update on CC RF noise and operational aspect”, presented at the 96th HiLumi WP2 Task Leader Meeting, Tuesday, 13 June 2017, <https://indico.cern.ch/event/645814/>
- [8] R. Bruce, *et al.*, “Updated parameters for HL-LHC aperture calculations for proton beams”, Rep. CERN-ACC-2017-0051, 2017.
- [9] H. Mainaud Durand *et al.*, “HL-LHC Alignment Requirements and Associated Solutions”, presented at the 8th Int. Particle Accelerator Conf. (IPAC17), Copenhagen, Denmark, May 2017, paper TUPIK085.
- [10] O. Brüning (ed.) *et al.*, “LHC Design Report”, Geneva, Switzerland, Rep. CERN-2004-003-V-1, Jun. 2004.